

Development and Characterization of Silicon Micromachined Nozzle Units for Continuous Ink Jet Printers

Lars Palm,[▲] Lars Wallman, Thomas Laurell, and Johan Nilsson[▲]

Department of Electrical Measurements, Lund Institute of Technology, Lund, Sweden

The design of a silicon micromachined nozzle unit to be used in continuous ink jet printers is suggested and characterized. A truncated pyramid shaped nozzle geometry was obtained by anisotropic etching and p-n junction etch stop processing of <100> silicon wafers. The pyramid shaped nozzle, with the exit on the front side of the silicon die, has a square orifice, which connects to the center of a 10 mm × 0.7 mm × 30 μm (L × W × D) channel situated on the backside of the die. The channel was sealed by an anodically bonded glass lid, which provided in- and outlet via drilled holes. The flow through option, given by the connection of the in- and outlet to each end of the channel, facilitates cleaning at the end of the manufacturing process as well as de-clogging of the nozzle during operation. The stimulation of the jet, to attain constant droplet size and distance between droplets, was achieved with the aid of a piezoelectric element that was glued to the glass lid on the backside of the nozzle unit. The piezoelectric element was positioned adjacent to the orifice of the nozzle to secure a good acoustic coupling to the jet. A jet emerged from a nozzle (10 μm × 10 μm orifice) with a velocity of 50 m/s at a flow rate of 0.22 ml/min when a pressure of 10 bar was used to force the ink through the nozzle unit. The droplet flight stability was characterized by an in-house developed optical measurement system. The results showed that the nozzle unit generated droplets with high droplet flight stability (less than 15° standard deviation in droplet period width measured at 7 mm from the orifice) in a large stimulation frequency region around the desired frequency of 1 MHz.

Journal of Imaging Science and Technology 44: 544–551 (2000)

Introduction

The nozzle is the essential element in applications where fluids are to be ejected as droplets. In order to attain the desired size of droplets with the desired droplet intervals, the nozzle unit must be carefully selected. The geometrical design naturally influences the performance of a nozzle concerning flow and droplet formation.^{1–8} For a specific application like ink jet printing, it is essential that the size and performance of the nozzle is identical over time and from unit to unit.

An application that demands both equally sized droplets and a constant time between droplets is the continuous ink jet printer.⁹ This printer uses droplets that have a diameter around 15 μm which are created at a rate of approximately 1 MHz.

The nozzles that are used in continuous ink jet printers are traditionally made by glass. The manufacturing of such a nozzle is a craftsmanship which can either be made by heating and pulling a glass tube (Siemens–Elema, Solna, Sweden) or made by heating and collapsing a glass tube.¹⁰ The commercially available printers often use glass nozzles with circular orifices with a diameter of 10 μm. In order to stabilize droplet formation, mechanical vibrations are applied to the nozzle.

Commonly a piezoelectric crystal supplies the external mechanical stimulation. Due to the complex mechanical resonance in the nozzle unit, the droplet flight stability varies when the stimulation frequency is varied.¹¹ Therefore, the manufacturing of large numbers of nozzles that should have identical performance in droplet generation is difficult.

One alternative to mass produce nozzles with repeatable performance is to use silicon micromachining.¹² Anisotropic etching of <100> silicon wafers facilitates the manufacturing of pyramid formed holes resulting in nozzles with well defined square orifices.^{13–17}

The use of silicon micromachined nozzles for continuous ink jet printers has been reported in Refs. 18 and 19. However no data has been reported on their ability to produce stable droplet trains with constant inter droplet distances which is a rudimentary demand.

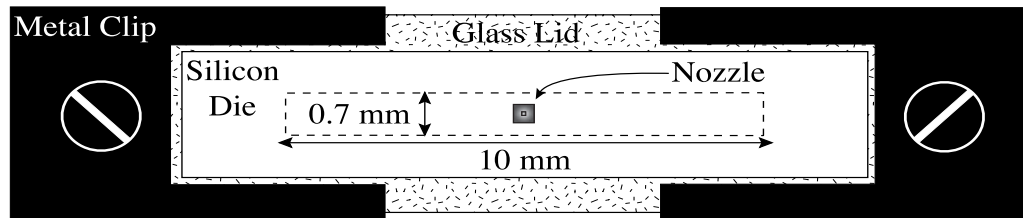
The goal is to produce a high quality printout for the continuous ink jet printer application. The droplets that hit the media on the rotating drum form the print. The matching of the drum rotation to the jet flow sets the color gamut. Typically, this is achieved by depositing droplets on the media at a rate of 1 MHz (droplet size ≈ 15 μm, ink flow ≈ 0.22 ml/min). The media has a typical surface velocity of 4 m/s when the resolution of the printer is ten lines per mm. If the nozzle orifice size is altered given the stipulated surface velocity, it is essential to maintain the flow if the same color gamut is intended. A consequence of a reduced nozzle orifice size at the given flow is that the number of droplets per time unit must be increased. A higher stimulation frequency must therefore be selected. On the other hand, if the

Original manuscript received April 10, 2000

▲ IS&T Member

©2000, IS&T—The Society for Imaging Science and Technology

Front View



Side Cut Away View

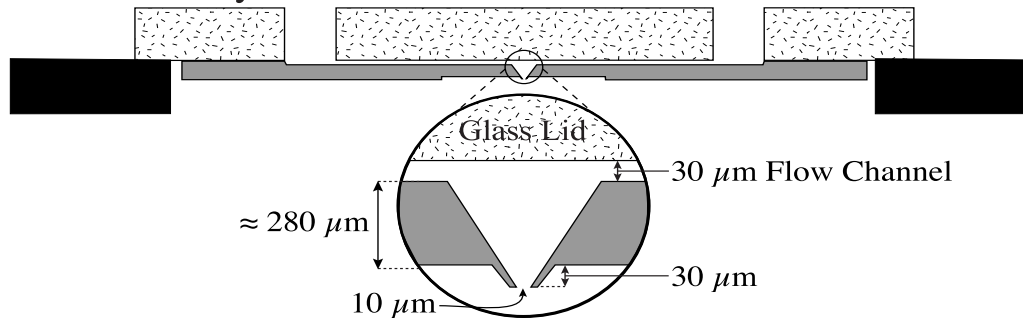


Figure 1. A cut away view of the nozzle structure. The dimensions for the flow channel in the nozzle prototype are (l) 10mm, (w) 0.7 mm and (d) 30 μm . The water-jet drilled holes in the glass lid have a diameter of approximately 1 mm. The glass lid is larger than the silicon die since the nozzle unit is mounted in the nozzle holder with metal clips that hold the nozzle unit in place by fixing the glass lid.

nozzle orifice size is increased with maintained flow the rate at which droplets are created must be reduced.

Smaller droplets reduce of the size of the smallest dot on the media and increase the number of steps in the halftoning but they are also more sensitive to air drag. Larger droplets are less affected by air drag but on the other hand the smallest possible dot on the media increases. The spot size used today in the printer is a compromise between these desires.

The micromachined prototype nozzle units described in this article were aimed to have well defined small orifice sizes (approximately $10 \times 10 \mu\text{m}$). The front area was kept as small as possible to minimize the risk of depositions of ink around the nozzle orifice which may cause directionality problems. A flow through channel was utilized to facilitate flushing of the nozzle unit after assembly in order to remove debris without forcing it through the nozzle orifice.

Measurements with the in-house developed optical measurement set up¹¹ showed that the suggested nozzle unit design has excellent performance in a wide frequency range around the desired 1 MHz stimulation frequency.

Materials and Methods

Nozzle Fabrication

The nozzle unit consists of a silicon microstructured die and a glass lid that is anodically bonded together.²⁰ The structure of the nozzle unit is shown in Fig. 1. The die houses a recessed truncated pyramid shaped nozzle and an ink flow channel. The glass lid serves as a backing for the flow channel and provides the flow channel with the ink inlet and outlet through two water jet drilled holes ($\varnothing \approx 1 \text{ mm}$). The nozzle unit is mounted in a nozzle holder as shown in Fig. 2. The holder houses a 1 μm PTFE in-line filter for the ink inlet. The holder also provides connections for the ink inlet and outlet hoses.

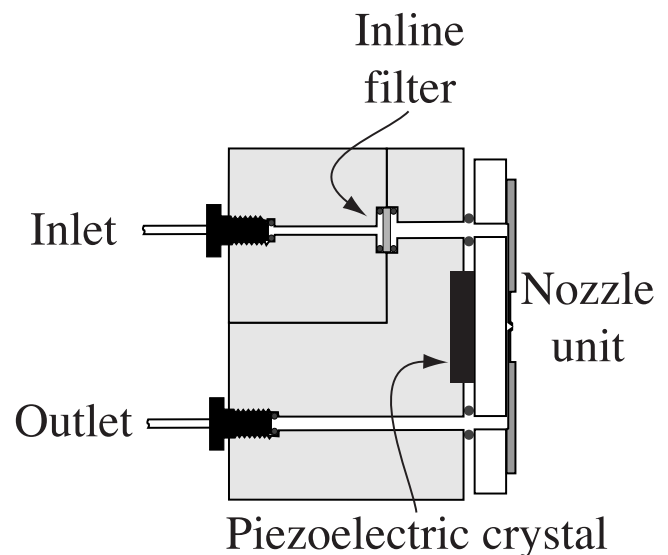


Figure 2. A cut away view of the nozzle unit holder.

The microstructures were etched in 3" $\langle 100 \rangle$ p-type (boron) silicon wafers using standard procedures of photolithography and wet etching steps. Negative photo resist was used to define the pattern in the silicon dioxide which was used as masking material throughout the processing. The silicon dioxide was patterned using buffered HF. Bulk etching of the patterned silicon wafer was performed in a KOH solution (160 g KOH / 500 ml H_2O). The wafers were mounted in an in-house built rotating wafer holder during etching to keep the etch-rate approximately constant across the wafer surface. The KOH etch beaker was immersed in a thermostated ultrasonic bath (Sonorex Super Digital 10P, Bandelin, Germany)

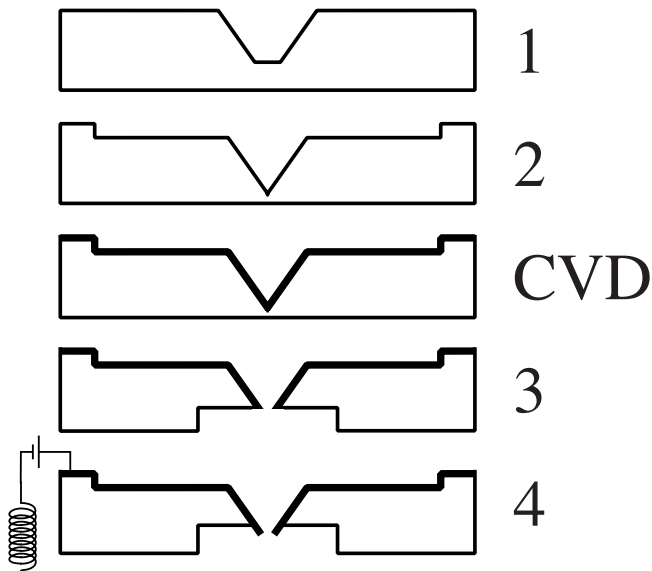


Figure 3. (1) The first mask and etching defines the base of the pyramid on the back of the wafer and begins the etching of the pyramid. (2) The second mask defines the position of the flow-channel surrounding the base of the pyramid. The second etching continues the etching of the pyramid and etches the channel to the desired depth. (CVD) After the second etch pass the backside of the wafer is doped using phosphor - thick line (3) The third mask and etching removes the silicon surrounding the nozzle from the front side of the wafer with anisotropic etching followed by p-n junction etch stop etching. The wafer is anisotropically etched from the front side until the orifice has the desired dimensions (4) The p-n junction etch stop is turned on for the time it takes to reveal the desired nozzle-height (appx. 30 μm) at the front side of the wafer.

to keep the KOH solution at a temperature of 70°C and to remove gas bubbles efficiently from the etch areas. Prior to the p-n junction etch stop process²¹ the wafers were phosphorous doped using a conventional CVD process.

The recessed pyramid shaped nozzle and the flow channel are constructed during four etchings that are explained in Fig. 3.

The silicon wafer is sawed into dice in which each contains a nozzle with a flow channel. A glass lid is anodically bonded on each of the nozzle dice so that the through-holes in the glass lid are positioned at each end of the flow channel as shown in Fig. 4. This construction enables the nozzle unit to be flushed with a cleaning fluid to remove any particles that are left in the flow channel during the manufacturing process without forcing them through the nozzle. After flushing the system, the outlet hole in the glass lid is closed with a removable seal.

To assure good acoustic coupling of the stimulation signal to the surface of jet of the piezoelectric crystal (Ferroperm A/S, Kvistgaard, Denmark) is glued onto the backside of the glass lid adjacent to the orifice of the nozzle.

Inkjet Characterization

To assess the droplet formation stability for the suggested nozzle unit, an optical measurement setup developed in house,¹¹ was utilized. The standard deviation for a large number of droplet-to-droplet periods was used as a measure of droplet flight stability (D.F.S.).

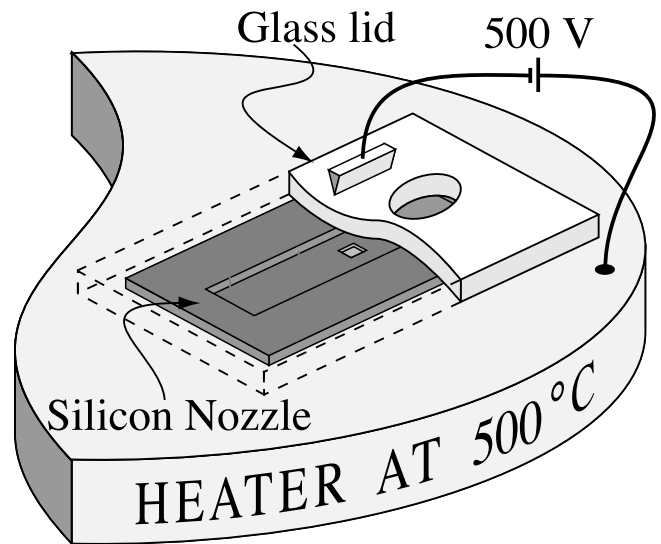


Figure 4. Anodic bonding of the silicon die and the glass lid. The through holes in the glass lid are positioned at the ends of the flow channel in the silicon die.

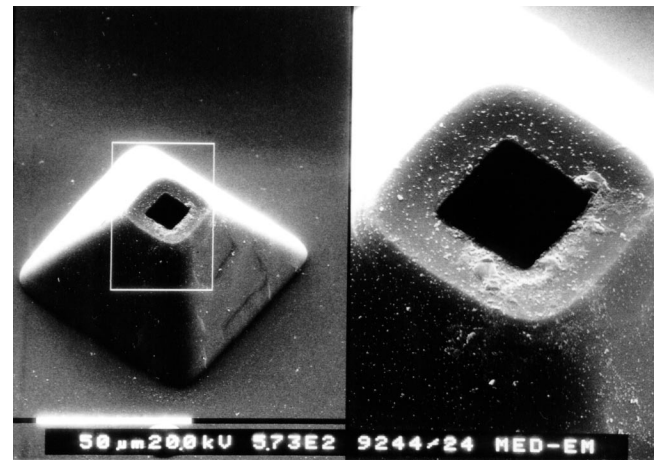


Figure 5. A top view micrograph of the nozzle captured in a SEM. The orifice size is approximately 10 \times 10 μm . The small front area in combination with the pyramid-shaped nozzle reduces the risk of misalignment of the jet due to deposition of ink close to the orifice.

The optical measurement set up was used to study the impact on droplet flight stability by the use of different stimulation frequencies. Experiments were conducted with constant amplitude (20 Vpp) of the stimulation signal while the frequency of the signal was altered in 20 kHz steps to scan the investigated frequency region (800 to 1200 kHz). The investigated frequency region was selected because it contains the natural droplet formation frequency for a nozzle with a circular orifice diameter of approximately 10 μm and a jet velocity of approximately 50 m/s. These are the typical operational parameters of the printers available today.

Results and Discussion

A top view of a silicon nozzle with an orifice of 10 \times 10 μm can be studied in Fig. 5.

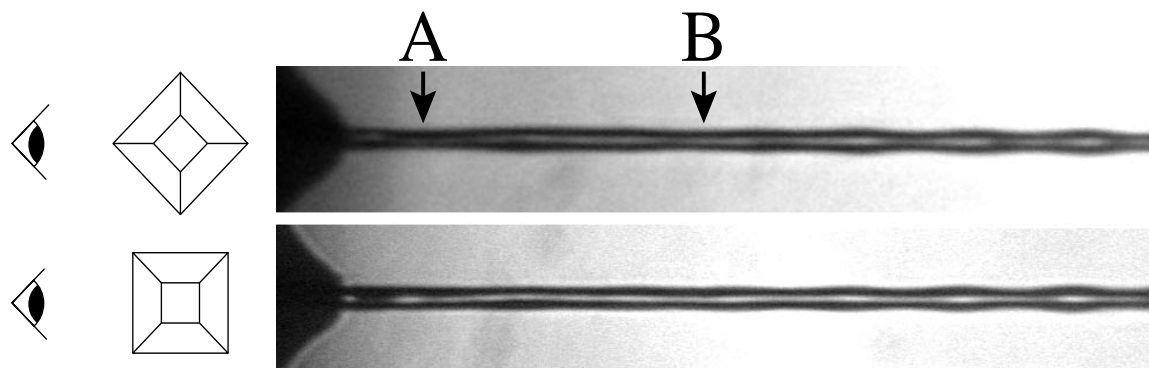


Figure 6. (Top) An image of the jet captured with the nozzle unit tilted 45° degrees to study the influence of the orifice corners. (Bottom) An image of the jet captured at a 0° angle to compare to the image of the tilted nozzle. It can be observed in these images that a jet ejected from square orifice changes to cylindrical shape very close to the orifice. This can be seen as the waves on the jet close to the nozzle (A). The small, imposed waves that cause break-up of the jet grow as the jet travels and are not clearly visible until position B.

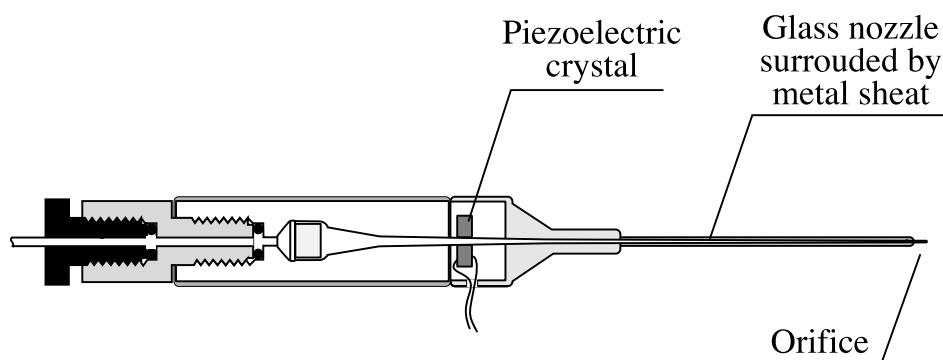


Figure 7. A cut away view of a glass nozzle (Siemens-Elema, Solna, Sweden). The ring-shaped piezoelectric crystal is glued to the glass nozzle.

The use of a square orifice results in a non-circular cross-section of the jet close to the orifice. However, these disturbances fade out before the wave that causes break up of the jet is visible on the surface [see Fig. 6]. The measured droplet flight stability for the silicon nozzles indicate that the droplet formation stability is high despite the non-cylindrical initial jet shape.

Glass nozzles studied earlier with our optical measurement set up have been found to have high droplet flight stability in frequency intervals or at individual frequencies.¹¹ The frequencies at which one glass nozzle operated satisfactorily was not correlated to the frequencies that another nozzle unit operated satisfactorily. A small increase or decrease of the frequency of the stimulation signal could change the stability from high to low or from low to high. The system could be adjusted to operate at frequencies that result in high droplet flight stability, but the main disadvantage with the glass nozzle is the variation of droplet flight stability, at a given frequency, from unit to unit. The piezoelectric element is glued to the glass nozzle quite far from the orifice as shown in Fig. 7, and this position influences the nozzle unit frequency behavior. Because the glass nozzle unit is constructed of several parts that all influence the units frequency behavior, it is difficult to foresee the high level of droplet flight stability frequencies at which the unit operates.

Measurements conducted with the optical measurement set up for silicon nozzle units showed that the drop-

let flight stability, for a wide range of stimulation frequencies, was better than that of a glass nozzle working at a stimulation frequency with high droplet flight stability.

A nozzle unit with an orifice of 10 μm in square driven by a pressure of 10 bar gives rise to a volume flow of 0.22 ml/min. The pressure needed to eject a jet from a glass nozzle with approximately the same exit area as the 10 μm silicon nozzle is around 40 bar. The pressure loss in a silicon nozzle is substantially less than for the glass nozzle. The ejected jet travels with a velocity of approximately 50 m/s. The result of droplet flight stability measurements conducted at 7 mm distance from the orifice can be studied in Fig. 8. The frequency behavior for the two nozzles (A and B) are similar which suggests that the variation of frequency behavior from nozzle unit to nozzle unit is substantially reduced compared to the glass nozzles.

The silicon nozzles have been studied in detail for two orifice sizes $7.5 \times 7.5 \mu\text{m}$ and $9.5 \times 9.5 \mu\text{m}$. These nozzles have orifice areas slightly smaller ($56 \times 10^{-12} \text{m}^2$) and slightly larger ($90 \times 10^{-12} \text{m}^2$) than the 10 μm circular orifice glass nozzle ($78 \times 10^{-12} \text{m}^2$). Storage fluid (Siemens-Elema, Solna, Sweden) was used as fluid in all experiments. The jet velocity, flow, and droplet flight stability for different frequencies was measured for pressures between 6 bar and 20 bar for the $7.5 \times 7.5 \mu\text{m}$ nozzle and between 8 bar and 22 bar for the 9.5×9.5

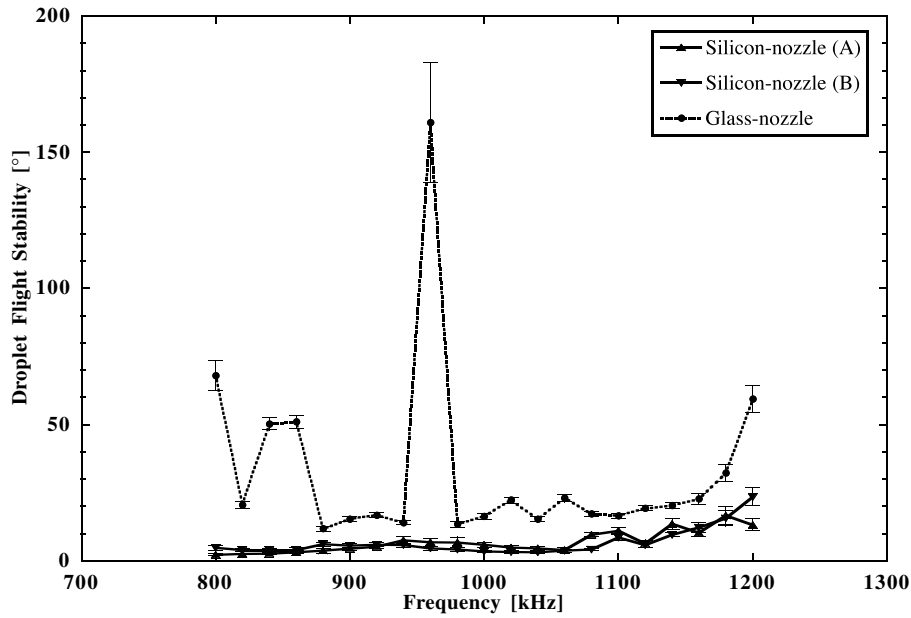


Figure 8. A study of droplet flight stability for two $10 \times 10 \mu\text{m}$ silicon nozzles and one glass nozzle ($\varnothing \approx 10\mu\text{m}$). All measurements are conducted at a distance of 7 mm from the orifice. All nozzles were operated at a flow of 0.22 ml/min, which was achieved at a pressure of 10 bar for the silicon nozzles and 40 bar for the glass nozzle. The stimulation frequency was varied from 800 to 1200 kHz. The error bars show the standard deviation for 500 consecutive droplet.¹¹ The measured droplet flight stability for the glass nozzle varies when the frequency is altered. An extremely bad stimulation frequency was detected at 960 kHz for the glass nozzle.

TABLE I. Flow and Jet Velocity as a Function of the Driving Pressure for the 7.5 and 9.5 μm Nozzles. The Theoretical Natural Droplet Formation Frequency (f_{natural}) and the Maximum Droplet Formation Frequency (f_{max}) Calculated from the Given Dimensions and Velocities Are Presented in Columns f_{natural} and f_{max} Respectively

Pressure [bar]	Flow [ml/min]		Velocity [m/s]		f_{natural} [kHz]		f_{max} [kHz]	
	7.5 μm	9.5 μm	7.5 μm	9.5 μm	7.5 μm	9.5 μm	7.5 μm	9.5 μm
6	0.08		26.7		699		1004	
8	0.09	0.21	30.0	32.0	786	662	1128	950
10	0.10	0.25	35.3	37.5	925	776	1327	1114
12	0.11	0.26	40.0	40.0	105	827	1505	1188
14	0.12	0.28	42.9	44.0	1124	910	1614	1307
16	0.13	0.30	46.1	47.0	1208	972	1734	1396
18	0.13	0.33	50.0	50.0	1310	1034	1881	1485
20	0.14	0.35	52.9	53.0	1386	1096	1990	1574
22		0.36		55.0		1138		1633

μm nozzle. From these measured values, the natural droplet formation frequency and maximum droplet formation frequency were calculated. Both the natural and the maximum droplet formation frequency are functions of the jet diameter (nozzle orifice size) and the jet velocity (see following equations) as well as liquid parameters like surface tension, viscosity and density.

$$f_{\text{natural}} = \frac{v_{\text{jet}}}{4.51 \cdot d_{\text{jet}}}$$

$$f_{\text{max}} = \frac{v_{\text{jet}}}{\pi \cdot d_{\text{jet}}}$$

The droplet flight stability measurement results for both orifice sizes are shown in Fig. 9. For driving pressures 6 and 8 bar the maximum droplet frequency is below the maximum stimulation frequency applied for the $7.5 \times 7.5 \mu\text{m}$ nozzle. The $9.5 \times 9.5 \mu\text{m}$ nozzle at driving pressures 8 to 12 bars also result in maximum

droplet formation frequencies lower than the maximum applied stimulation frequency. This is evident in Fig. 9 where the measured droplet flight stability decreases to a great extent when the stimulation frequency is increased above the respective maximum frequency. The low droplet flight stability for the two lowest pressures at 840 kHz is probably due to an undesired resonance in the nozzle unit. When observed in stroboscopic light the droplets had formed pairs indicating the presence of two different droplet velocities in the droplet train.

For the $7.5 \mu\text{m}$ nozzle unit, the driving pressure 6 bar results in maximum droplet frequencies below the normal stimulation frequency of 1 MHz, hence this driving pressure is excluded from the following investigations for this nozzle. Likewise, the driving pressures below 12 bar are excluded for the $9.5 \mu\text{m}$ nozzle unit.

The principle for the continuous inkjet printer is based on the possibility to charge and deflect unwanted droplets. In order to charge and deflect droplets correctly the charge pulses must be applied in correct phase

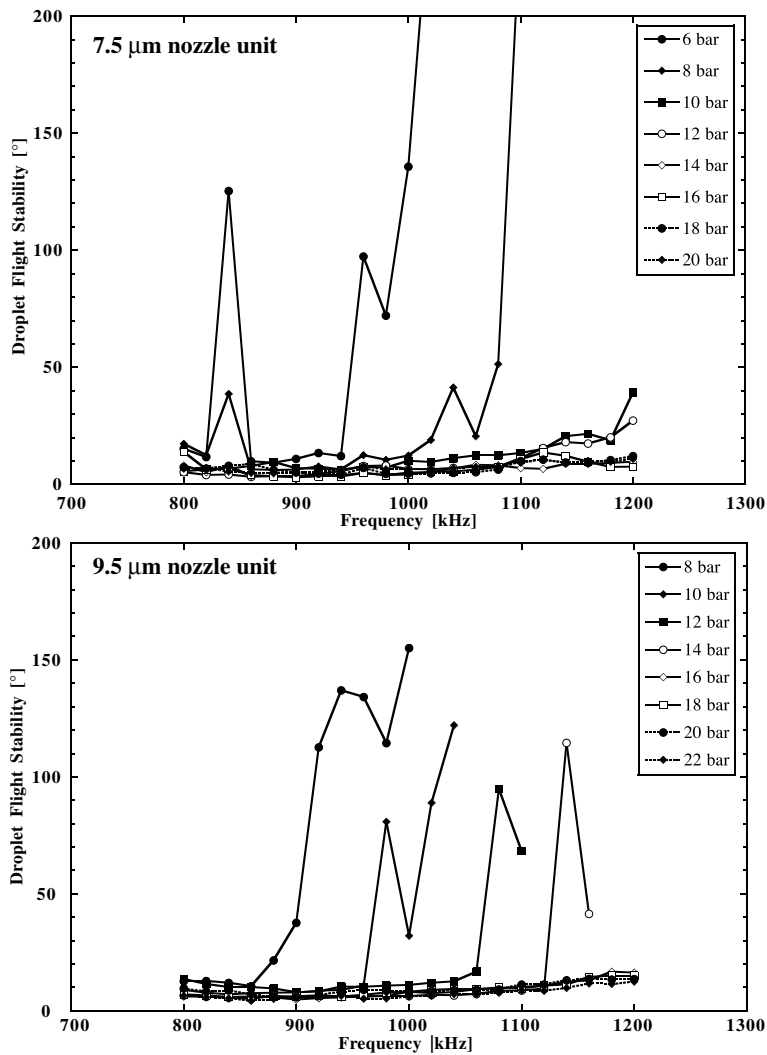


Figure 9. Droplet flight stability as a function of stimulation frequency for the two nozzle units measured at a distance of 7 mm from the orifice. (7.5 μm) The dramatic decrease in droplet flight stability for the 6 and 8 bar driving pressure measurements when the stimulation frequency is approaching 1 MHz respectively 1.1 MHz is due to the maximum droplet formation frequencies. (Table I). When a stimulation frequency above the maximum droplet formation frequency is applied to the nozzle no controlled droplet break up occur and the droplet flight stability is very low (9.5 μm). The influence of the maximum droplet formation frequencies (Table I) can be observed for driving pressures up to 14 bar.

relationship with the droplet formation process.⁹ In order to make a complete assessment of whether the droplet formation can be used for printing or not, the charging/discharging of the droplets through the jet connected to ground potential in the nozzle unit must also be evaluated.

The electrical resistance to the tip of the jet is strongly influenced by the diameter of the jet. As the jet travels from the orifice, the amplitude of the applied periodical mechanical disturbances grow exponentially (see Fig. 10). The filament closest to the droplet to be cut off gives the major contribution to the resistance. The resistance has its lowest value just after the preceding droplet is cut off and in order to be able to fully charge a droplet the charging should be started at this time.^{22–25} It is however possible to fully charge a droplet even if the charging is begun after the resistance is as low as possible. The maximum delay time that still results in fully charged droplets, defines the allowed zone for the charging of

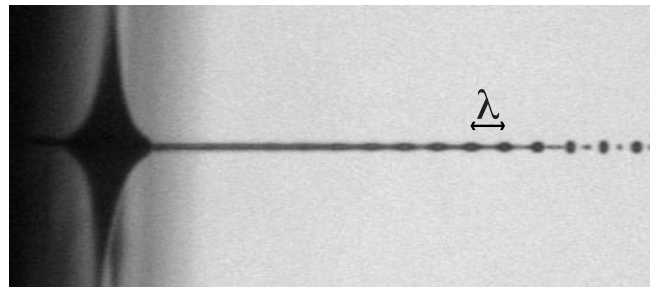


Figure 10. A jet ejected from a 7.5 μm silicon nozzle captured in stroboscopic light. The distance to the point of droplet formation is approximately 0.5 mm and the jet velocity is 45 m/s. The stimulation signal has a period of 1 μs. Due to the applied stimulation the jet breaks up into droplets in a controlled manner. As the break-up progresses the resistance to the tip of the jet will increase as a result of the decreasing filament thickness.

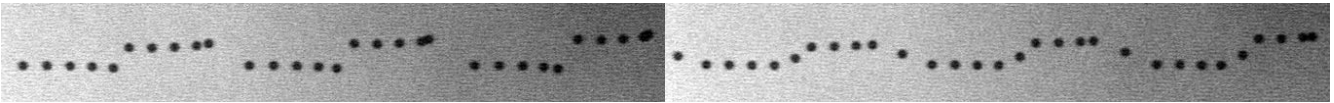


Figure 11. The droplets in both images are travelling from left to right (Left). The upper five droplets are correctly positively charged and the lower five droplets are uncharged. The first droplets in the charged set are given a slightly higher charge than the other charged droplets since the charge of the following droplets will be repelled by the charge in these droplets. Correspondingly the first uncharged droplet is given a slight negative charge due to the historic effect.⁹ The phase difference between stimulation signal and charge pulse is within the allowed zone (Right). In this image the phase difference between charge pulse and stimulation is not within the allowed zone. The droplet that is positioned between the charged droplets and the uncharged droplets has been given an undesired level of charge.

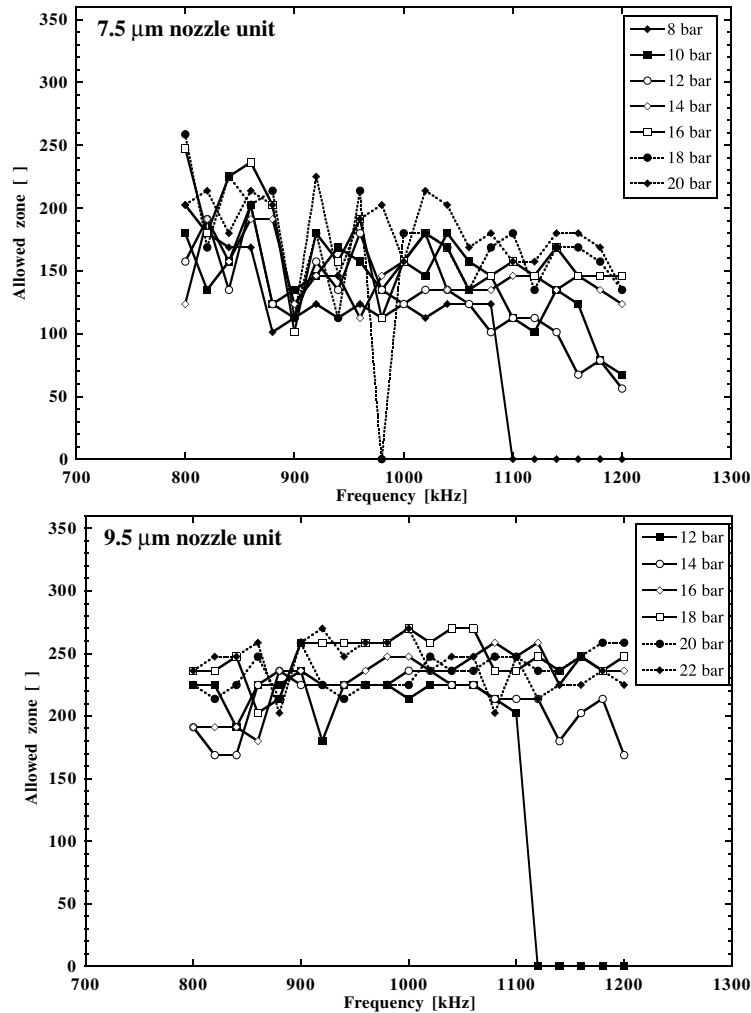


Figure 12. (7.5 μm) Allowed zone for the $7.5 \times 7.5 \mu\text{m}$ nozzle measured at driving pressures 8 to 20 bar in the frequency interval 800 to 1200 kHz. (9.5 μm) The allowed zone for the $9.5 \times 9.5 \mu\text{m}$ nozzle measured at driving pressures 12 to 22 bar for the same frequency interval as for the $7.5 \times 7.5 \mu\text{m}$ nozzle.

droplets.⁹ The allowed zone is expressed in degrees to relate to the period of the stimulation signal. In printing applications it is essential that the allowed zone is wide enough to allow for some drift in the phase relationship between the droplet cut off and the charging signal. The phase relationship is normally adjusted at periodic intervals, e.g., once per revolution of the printer drum.

High droplet flight stability does not necessarily lead to a large allowed zone. Processes at droplet cut off, like satellite droplet formation, may decrease the allowed zone width to the amount where the droplet formation can no longer be used in a printer. To determine the

charging performance for the silicon nozzle units the phase for the charge pulse is shifted 360° in 32 steps compared to the phase of the stimulation signal. The droplet train is divided into groups of 10 droplets. For each of these groups, a group of five consecutive droplets are charged and the remaining five droplets are left uncharged. When the charge pulse is applied to the jet within the allowed zone all five charged droplets will hence be deflected in the same manner [see Fig. 11 (left)]. If the phase difference is too large droplets will be charged to intermediate levels and all charged droplets are no longer deflected in the same manner [see Fig. 11 (right)].

The allowed zone for driving pressures 8 to 20 bar was studied for the $7.5 \times 7.5 \mu\text{m}$ nozzle unit and the pressures used for the $9.5 \times 9.5 \mu\text{m}$ nozzle unit was 12 to 22 bar. The results are shown in Fig. 12. The small allowed zone for 18 bar driving pressure for the $7.5 \mu\text{m}$ nozzle unit at 980 kHz is due to the presence of slow merging satellite droplets. These satellites merge with the main droplet after some time of flight and their presence cannot be detected in the droplet flight stability measurement presented in Fig. 9 but their influence on the allowed zone is obvious. The driving pressure 8 bar ($7.5 \mu\text{m}$ nozzle unit) and 12 bar ($9.5 \mu\text{m}$ nozzle unit) resulted in low droplet flight stability when the stimulation frequency was set above 1100 kHz. For these stimulation frequencies, the allowed zone was reduced to zero because the charging of the droplets was obstructed by the unsynchronized droplet formation. The allowed zone for most frequencies and pressures for the $7.5 \times 7.5 \mu\text{m}$ nozzle unit was found to be around 150° . The allowed zone for the $9.5 \times 9.5 \mu\text{m}$ unit is larger than for the $7.5 \times 7.5 \mu\text{m}$ nozzle which can be explained by the larger jet diameter which in turn results in decreased electrical resistance in the jet. For this nozzle, the allowed zone is around 225° throughout the frequency interval for most driving pressures.

A larger nozzle will give rise to a larger jet diameter and the resistance to the tip of the jet will be reduced. The filament connecting the droplet that is about to be cut off to the jet gives the largest contribution to the resistance. The diameter of the filament is related to the diameter of the jet and therefore the largest resistance will be less for the $9.5 \times 9.5 \mu\text{m}$ nozzle than for the $7.5 \times 7.5 \mu\text{m}$ nozzle. This increases the size of the allowed zone as can be seen in Fig. 12.

The use of silicon nozzles in continuous ink jet printers is possible since the droplet flight stability for jets from silicon nozzles with the suggested design is superior to that of a glass nozzle for a given frequency. The silicon nozzles show very high droplet flight stability ($<15^\circ$ D.F.S.) for the entire studied frequency interval unless the maximum droplet formation frequency is exceeded by the stimulation frequency.

The design of the silicon nozzle unit with its pyramid shape has proven mechanically rugged for withstanding repeated cleaning with a cleaning tissue. The fact that the nozzles are recessed below the wafer front surface (cf. Fig. 3) also protects them from mechanical damage.

The flow through design has shown advantageous both during manufacturing and during operation. Experiments have shown that it is possible to open clogged nozzles by applying suction to the opened outlet while the inlet is closed. The inlet is thereafter opened, allowing ink to flow into the nozzle unit while the suction is still applied to the outlet.

An advantage for the silicon nozzles compared to the glass nozzles is the ease of manufacturing and further the possibility to put nozzles in close proximity of each other. Small distances between nozzles are vital if nozzle systems with multiple nozzles per color are to be developed. With the suggested method of manufacturing nozzles it is not possible to position the nozzles close enough to generate one-pass printouts with high resolution. The printing still has to be completed in multiple passes but the printout time will be substantially reduced.

Conclusions

The suggested silicon nozzle is very well suited to be used in continuous inkjet printers because it is capable of producing uniformly sized droplets with highly constant intervals. Due to the choice of design, the desired flow can be maintained with much lower driving pressure than for the glass nozzle.

The stimulation frequency can be varied in the interval of 800 to 1200 kHz without any change in measured droplet flight stability given that the nozzle unit is operated around the natural droplet formation rate. The silicon nozzles were found to have large allowed zones, which facilitates printing. The design is well suited for development of multiple nozzle units. ▲

References

1. I. W. S. Rayleigh, On the instability of jets, *Proc. London Mathematical Society*, **10**, 4–13 (1879).
2. M. J. McCarthy and N.A. Molloy, Review of stability of liquid jets and the influence of nozzle design, *Chem. Eng. J.* **7**, 1–20 (1974).
3. S. A. Curry and H. Portig, Scale Model of an Ink Jet, *IBM J. Res. Dev.* **21**(1), 10–20 (1977).
4. M. Levanoni, Study of Fluid-Flow Through Scaled-Up Ink Jet Nozzles, *IBM J. Res. Dev.* **21**(1), 56–68 (1977).
5. D. B. Bogoy, Drop Formation in a Circular Liquid Jet, *Annual Review of Fluid Mechanics* **11**, 207–228 (1979).
6. J. H. Lienhard, Velocity Coefficients For Free Jets From Sharp-Edged Orifices, *Mech. Eng.* **106**(5), 93–93 (1984).
7. B. Lopez, A. Soucemarianadin and P. Atané. The role of nozzle geometry on the break-up of liquid jets. in *Proc. IS&T's NIP 13, Int'l. Cong. on Digital Printing Technologies*, IS&T, Springfield, VA, 1997, 609–614.
8. R. V. Lorenze and D. E. Kuhman, Correlation of misdirected satellite drops and resultant print quality defects with nozzle face geometries in thermal ink jet printheads, *J. Imaging Sci. Technol.* **39**(6), 489–494 (1995).
9. C. A. Hertz and B. A. Samuelsson, Ink Jet Printing of High Quality Color Images, *J. Imaging Sci. Technol.* **15**(3), 141–148 (1989).
10. D. B. West, A nozzle of a fluid dispensing device, *Eur. Pat. 588618A2*, (1994).
11. L. Palm and J. Nilsson, An optical method for measuring drop flight stability in a continuous ink jet, *J. Imaging Sci. Technol.* **41**(1), 48–53 (1997).
12. K. E. Petersen, Silicon as a Mechanical Material, *Proc. of the IEEE* **70**(5), 420–457 (1982).
13. E. Bassous, H. H. Taub and L. Kuhn, Ink Jet Printing Nozzle Arrays Etched in Silicon, *Appl. Phys. Lett.* **31**(2), 135–137 (1977).
14. E. Bassous and E. F. Baran, The Fabrication of High Precision Nozzles By the Anisotropic Etching of (100) Silicon, *J. Electrochemical Society* **125**(8), 1321–1327 (1978).
15. M. Tamai, Formation of a multi-nozzle ink jet, *US. Pat. 4455194*, (1984).
16. H. A. Waggner and J. C. Zuercher, Silicon Nozzle structures and method of manufacture, *US. Pat. 4733823*, (1988).
17. J. H. Babaei, C. Y. Kwok and R. S. Huang, An integrable nozzle for monolithic microfluid devices, *Sensors and Actuators (a)*, **65**, 221–227 (1998).
18. L. Smith, A. Soderberg and U. Bjorkengren, Continuous Ink-Jet Print Head Utilizing Silicon Micromachined Nozzles, *Sensors and Actuators A-Physical*, **43**(1–3), 311–316 (1994).
19. T. Diepold, E. Obermeier and A. Berchtold, A micromachined continuous ink jet print head for high-resolution printing, *J. Micromechanics and Microengineering* **8**(2), 144–147 (1998).
20. G. Wallis and D.I. Pomerantz, Field Assisted Glass-Metal Sealing, *J. Appl. Phys.* **40**(10), 3946–3949 (1969).
21. W. Chong-ruo, An investigation on p-n junction etch stop, *Sensors and Actuators A* **35**, 181–187 (1993).
22. G. L. Fillmore, W. L. Buehner and D. L. West, Drop Charging and Deflection in an Electrostatic Ink Jet Printer, *IBM J. Res. Dev.* **21**(1), 37–47 (1977).
23. A. Atten and S. Oliveri, Charging of Drops Formed By Circular Jet Breakup, *J. Electrostatics* **29**(1), 73–91 (1992).
24. J. Nilsson, *Applications of Micro Drops*, Diss., Dept. of Electrical Measurements, Lund University, Sweden, ISRN LUTEDX/TEEM—1051—SE (1993).
25. W. D. Warnica, M. Vanreenen, M. Renksizbulut, and A. B. Strong, Charge synchronization for a piezoelectric droplet generator, *Rev. Sci. Instr.* **64**(8), 2334–2339 (1993).